NHS Breast Screening Programme

NHS
Cancer Screening Programmes

Technical evaluation of Hologic Selenia Dimensions 2-D Digital Breast Imaging System with software version 1.4.2

KC Young, JM Oduko

NHSBSP EQUIPMENT REPORT 1201

JULY 2012

Technical evaluation of Hologic Selenia Dimensions 2-D Digital Breast Imaging System with software version 1.4.2

NHSBSP EQUIPMENT REPORT 1201

July 2012

Authors

JM Oduko
KC Young
National Coordinating Centre for the Physics of Mammography, Guilford

Editor

Kiera Chapman
NHS Cancer Screening Programmes

Typesetting and Design

Mary Greatorex
NHS Cancer Screening Programmes

Published by
NHS Cancer Screening Programmes
Fulwood House
Old Fulwood Road
Sheffield
S10 3TH

Tel: 0114 271 1060
Fax: 0114 271 1089
Email: info@cancerscreening.nhs.uk
Website: www.cancerscreening.nhs.uk

The report is available in PDF format on the NHS Cancer Screening Programmes' website.

Version Control Technical evaluation of Hologic Selenia Dimensions 2-D Digital Breast Imaging System with software version 1.4.2			
Electronic publication date		July 2012	
Review date (1)		July 2013	
Review date (2)			
Comments		May be sent to Professor Ken Young, ken.young@nhs.net in readiness for review.	
Interim Amendments			
Version	**Description of change**	**Author**	**Date**

CONTENTS

ACKNOWLEDGEMENTS **iv**

1. INTRODUCTION **1**

1.1 Testing procedures and performance standards for digital mammography 1
1.2 Objectives 1

2. METHODS **2**

2.1 System tested 2
2.2 Output and half-value-layer (HVL) 3
2.3 Detector response 3
2.4 Dose measurement 3
2.5 Contrast-to-noise ratio (CNR) 4
2.6 AEC performance for local dense areas 5
2.7 Noise analysis 6
2.8 Image quality measurements 7
2.9 Image retention 8
2.10 Physical measurements of the detector performance 8
2.11 Optimisation 8

3. RESULTS **9**

3.1 Output and HVL 9
3.2 Detector response 9
3.3 AEC performance 10
3.4 Noise measurements 13
3.5 Image quality measurements 1
3.6 Comparison with other systems 4
3.7 Artefact 8

4. DISCUSSION **9**

5. CONCLUSIONS **9**

6. REFERENCES **10**

ACKNOWLEDGEMENTS

The authors are grateful to the staff at the Jarvis Breast Screening Centre, Guildford for their cooperation in evaluating the equipment at their site.

1. INTRODUCTION

1.1 Testing procedures and performance standards for digital mammography

This report is one of a series evaluating commercially available digital mammography systems on behalf of the NHS Breast Screening Programme (NHSBSP). The testing methods and standards applied are mainly derived from NHSBSP Equipment Report 0604, and are referred to in this document as 'the NHSBSP protocol.[1] The standards for image quality and dose within the NHSBSP protocol are the same as those of the European protocol, but the latter has been followed where it provides a more detailed performance standard: for example, for the automatic exposure control (AEC) system.[2,3]

1.2 Objectives

The purpose of these tests was to produce an update to NHSBSP report 1101[4] on the Dimensions Breast Imaging System, and to evaluate a software upgrade, Version 1.4.2, prior to its potential rollout in the NHSBSP in England. Two specific areas of the upgrade were considered:

(1) The new AEC table, designed to maintain a more constant contrast-to-noise ratio (CNR) at all breast thicknesses, resulting in an increase dose in cases where breast thickness is ≥ 5cm.

(2) The new software's ability to remove the artefacts that were associated with image processing in previous versions, e.g. dark areas around high contrast objects such as 'MRI coils'.

The tomographic performance of the system was not evaluated. Clinical evaluations are published separately by the NHSBSP where systems meet the minimum standards outlined in the NHSBSP protocol. A final decision on the suitability of systems for use within the NHSBSP depends on a review of both the technical and clinical evaluations.

2. METHODS

2.1 System tested

The tests were conducted at the Jarvis Breast Screening Centre in Guildford, on a Dimensions system installed in 2011 and described in Table 1. The system had been upgraded and the AEC curve had been adjusted to be as close as possible to the Hologic specifications.

Table 1, below, updates the data from the previously published report on the Hologic Selenia Dimensions[4] and contains some corrected values for added filtration and detector area.

Table 1 System Description

Manufacturer	Hologic Inc
Model	Dimensions
System serial number	81011100510
X-ray tube	Varian M-113T
Target material	Tungsten
Added filtration	50 µm Rhodium 50 µm Silver
Detector type	Amorphous selenium
Detector serial number	MM601656
Pixel size	70 µm (in detector plane)
Detector area	Small: 179 x 233 mm Large: 233 x 287 mm
Pixel array	Small: 2560 x 3328 Large: 3328 x 4096
Pixel value offset	50
Source to detector distance	700 mm
Source to table distance	675 mm
AEC modes*	AutoFilter, AutokV, AutoTime
AEC pre-exposure pulse	5 mAs for CBT < 5 cm; 10 mAs for CBT ≥ 5 cm
Software version(s)	AWS:1.4.2.246\M35:1.2.2.34\GIP2D:3.11.0-4.11.2\GIP3D:1.1.0.2\SNRCNR:1.0.0.0-1.0.1.0\PMC:1.4.2.2\DET:1.4.1.5\DTC:1.0.0.9\GCB:1.4.2.4GEN:1.4.2.0\VTA:1.4.0.15\CRM:1.4.2.0\THD:1.4.0.7\CDI:1.4.0.9\AIO:1.4.0.0\BKY:1.4.0.3

The AEC modes are as follows:

- AutoFilter: System selects kV, filter, and mAs. (Choice of kV and filter is based on compressed breast thickness).
- AutokV: User selects filter, system selects kV and mAs.
- AutoTime: User selects filter and kV, system selects mAs.

Position 2 was selected for all AEC measurements except the local dense area test, for which Auto was used.

In all cases, the pre-exposure pulse contributes to patient dose but does not contribute to the formation of the image. The pre-pulse is 5 mAs where compressed breast thickness is < 5 cm, and 10 mAs where breast thickness is > 5 cm.

2.2 Output and half-value-layer (HVL)

The output and HVL were measured in the manner described in the NHSBSP protocol, at intervals of 3 kV for each target/filter combination.

2.3 Detector response

The detector response was measured in the manner described in the NHSBSP protocol, with a 45 mm thickness of Perspex (polymethylmethacrylate, or PMMA) placed at the tube exit port. An ion chamber was positioned above the table, 4 cm in from the chest wall edge, to determine the incident air kerma at the detector surface for a range of manually set mAs values at 29 kV, and for both available target/filter combinations (W/Rh and W/Ag). The readings were corrected to the surface of the detector using the inverse square law. No correction was made for attenuation by the table and detector cover. Images were saved as unprocessed files and transferred to another computer for analysis. A 10 mm square region of interest (ROI) was positioned on the midline, 4 cm from the chest wall edge of each image. The average pixel value and the standard deviation of pixel values within that region were measured. The relationship between average pixel values and the detector entrance surface air kerma was determined.

2.4 Dose measurement

Doses were measured using the x-ray set's automatic exposure control (AEC) to expose different thicknesses of PMMA. Each thickness had an area of 18 x 24 cm. The paddle height was adjusted to be equal to the equivalent breast thickness. Mean glandular doses (MGDs) were calculated for the equivalent breast thicknesses. To measure the contrast-to-noise ratio (CNR), an aluminium square measuring 10 mm x 10 mm in area and 0.2 mm in depth was placed on top of a 20 mm thick block, with one edge on the midline, 6 cm from the chest wall edge. Additional layers of PMMA were placed on top of these to vary the total thickness.

2.5 Contrast-to-noise ratio (CNR)

The images of the PMMA blocks obtained during the dose measurement were analysed to obtain the CNRs. Twenty small square ROIs (approximately 2.5 mm x 2.5 mm) were used to determine both the average signal and the standard deviations in the signal within the image of the aluminium square (4 ROI) and its surrounding background (16 ROI), as shown in Figure 1. Small ROIs are used to minimise distortions resulting from the heel effect and other causes of non-uniformity.[5] This is less important for DR systems than for computed radiography systems, however, because a flat-field correction is applied. The CNR was calculated for each image, as defined in the NHSBSP and European protocols.

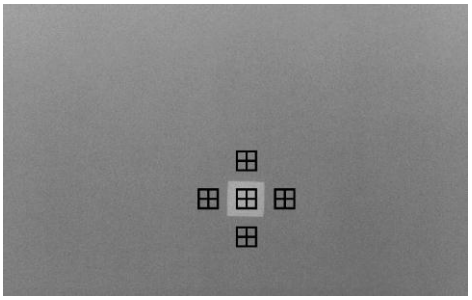

Figure 1 Location and size of ROI used to determine the CNR.

To apply the standards in the European protocol, the limiting value for CNR (using 50 mm PMMA) was determined according to Equation 1, below. This equation determines the CNR value ($CNR_{limiting\ value}$) that is necessary to achieve the minimum threshold gold thickness for the 0.1 mm detail (i.e. *threshold gold*$_{limiting\ value}$ = 1.68 µm which is equivalent to *threshold contrast*$_{limiting\ value}$ = 23.0%, using 28 kV Mo/Mo). Threshold contrasts were calculated in the manner described in the European protocol and in Equation 1.

$$CNR_{limiting\ value} = CNR_{measured} \times \frac{TC_{measured}}{TC_{limiting value}} \quad (1)$$

The relative CNR was then calculated according to Equation 2, and compared with the limiting values provided for relative CNR shown in Table 2. The minimum CNR required to meet this criterion was then calculated.

$$Relative\ CNR = CNR_{measured} / CNR_{limiting\ value} \quad (2)$$

Table 2 Limiting values for relative CNR

Thickness of PMMA (mm)	Equivalent breast thickness (mm)	Limiting values for relative CNR (%) in European protocol
20	21	>115
30	32	>110
40	45	>105
45	53	>103
50	60	>100
60	75	>95
70	90	>90

2.6 AEC performance for local dense areas

The method used in the EUREF type testing protocol was followed. To simulate local dense areas, nine images were made, and areas of extra attenuation of different thicknesses (2–18 mm) were added. The compression plate remained in position at a 40 mm height, as shown in Figure 2.

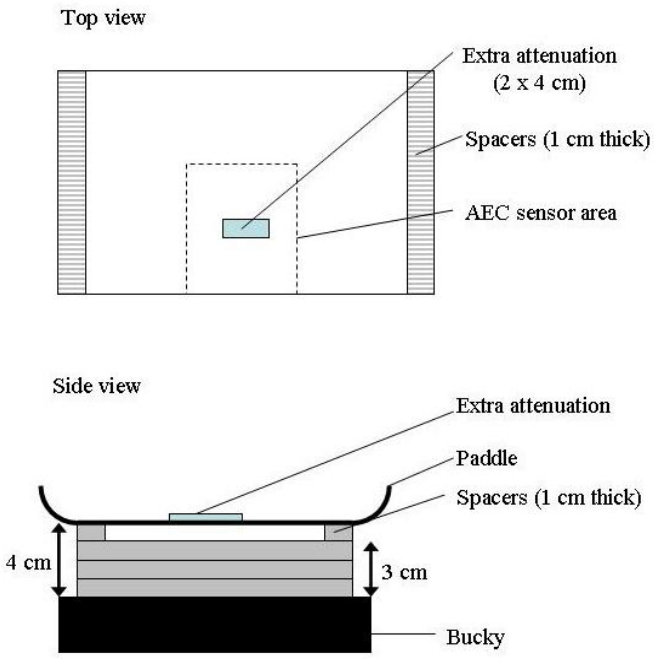

Figure 2 Setup to measure AEC performance for local dense areas

In the area of extra attenuation (20 x 40 mm PMMA), the mean pixel value and standard deviation were measured for a ROI with dimensions 2.5 x 2.5 mm, and the signal-to-noise ratio (SNR) calculated.

2.7 Noise analysis

The images acquired while measuring detector response using 29 kV W/Rh were used to analyse the image noise. A ROI, comprising an area of 5 x 5 mm was placed on the midline, 6 cm from the chest wall edge. This ROI was divided into four smaller ROI measuring 2.5 mm x 2.5 mm and the average standard deviations of the pixel values in these for each image were used to investigate the relationship between dose, detector, and image noise. It was assumed that this noise comprises three components – electronic noise, structural noise, and quantum noise – with the relationship shown in Equation 3:

$$\sigma_p = \sqrt{k_e^2 + k_q{}^2 p + k_s{}^2 p^2} \quad (3)$$

where σ_p is the standard deviation in pixel values within an ROI with a uniform exposure and a mean pixel value, p, and k_e, k_q, and k_s are the coefficients determining the amount of electronic, quantum, and structural noise in a pixel with a value, p.

This method of analysis has been described previously.[5] For simplicity the noise is generally presented here as relative noise, defined in equation 4.

$$Relative\ noise = \frac{\sigma_p}{p} \quad (4)$$

The variation in relative noise with mean pixel value was evaluated and fitted using Equation 3, and non-linear regression was used to determine the best fit for the constants and their asymptotic confidence limits (using GraphPad Prism Version 5 for Windows[*]). This established whether the experimental measurements of the noise fitted this equation, and the relative proportions of the different noise components. In fact, the relationship between noise and pixel values has been empirically found to be approximated by a simple power relationship, as shown in Equation 5.

$$\frac{\sigma_p}{p} = k_t p^{-n} \quad (5)$$

Here, k_t is a constant. If the noise were purely quantum noise the value of n would be 0.5. However the presence of electronic and structural noise means that n can be slightly higher or lower than 0.5.

The variance in pixel values within a ROI is defined as the standard deviation squared. The total variance was plotted against incident air kerma at the detector and fitted using Equation 3. Again, non-linear regression was used to determine the best fit for the constants and their asymptotic confidence limits, using the GraphPad Prism software.

[*] GraphPad Software, Inc, San Diego, California, USA, www.graphpad.com.

Using the calculated constants, the structural, electronic, and quantum components of the variance were estimated, assuming that each component was independently related to incident air kerma. The percentage of the total variance represented by each component was then calculated and plotted against incident air kerma at the detector. From this, the dose range over which the quantum component dominates was estimated.

2.8 Image quality measurements

Contrast detail measurements were made using a CDMAM phantom†, serial number 1022. The phantom was positioned with a 20 mm thickness of PMMA above and below, to give a total attenuation approximately equivalent to 50 mm of PMMA, or 60 mm of typical breast tissue. The kV target/filter combination and mAs were chosen to match as closely as possible to those selected by the AEC when imaging a 5 cm thickness of PMMA. This procedure was repeated to obtain a representative sample of 16 images at this dose level. Unprocessed images were transferred to disk for subsequent analysis off-site. Further images of the test phantom were then obtained at other dose levels by manually selecting higher and lower mAs values with the same beam quality. An automatic method of reading the CDMAM images was used.[6,7] The threshold gold thickness for a typical human observer was predicted using Equation 6.

$$TC_{predicted} = r\, TC_{auto} \quad (6)$$

$TC_{predicted}$ is the predicted threshold contrast for a typical observer, and TC_{auto} is the threshold contrast measured using an automated procedure with CDMAM images. Contrasts were calculated from gold thickness for a nominal tube voltage of 28 kV and a Mo/Mo target/filter combination (as described in the European protocol); r is the average ratio between human and automatic threshold contrast, determined experimentally with the values shown in Table 3.[7]

Table 3 Values of *r* used to predict threshold contrast

Diameter of gold disc (mm)	Average ratio of human to automatically measured threshold contrast (*r*)
0.08	1.40
0.10	1.50
0.13	1.60
0.16	1.68
0.20	1.75
0.25	1.82
0.31	1.88
0.40	1.94
0.50	1.98
0.63	2.01
0.80	2.06
1.00	2.11

† Version 3.4, UMC St. Radboud, Nijmegen University, Netherlands

The main advantage of automatic reading is that it has the potential to eliminate observer error, which is a significant problem when using human readers. However, it should be noted that at the present time, the official protocols are based on human reading.

The predicted threshold gold thickness for each detail diameter at each dose level was fitted with a curve, as described in the NHSBSP protocol. The confidence limits for the predicted threshold gold thicknesses had been previously determined via a resampling method, using a large set of images. The threshold contrasts quoted in the tables of results are derived from the fitted curves, as this has been found to improve accuracy.[6] The expected relationship between threshold contrast and dose is shown in Equation 7.

$$Threshold\ contrast = \lambda D^{-n} \quad (7)$$

D represents the MGD for a 60 mm thick standard breast, equivalent to the test phantom configuration used for the image quality measurement, and λ is a constant to be fitted. It is assumed that a similar equation applies when using threshold gold thickness, rather than contrast. This equation was plotted with the experimental data for each detail size from 0.1 to 1.0 mm. The value of n resulting in the best fit to the experimental data was determined.

2.9 Image retention

Not measured.

2.10 Physical measurements of the detector performance

Not measured.

2.11 Optimisation

Not performed.

2.12 Artefact evaluation

A small metal coil on a breast-like phantom was imaged, to verify that there no dark region was visible on the image around the coil (which would obscure calcifications, for example). Such dark areas had been observed on processed images with the previous software version. A line was drawn through the coil and surrounding area, and a profile was plotted. The image and profile were compared with those acquired prior to the upgrade.

3. RESULTS

3.1 Output and HVL

The results are shown in Table 4.

Table 4 Output and HVL

kV T/F	Output (mGy/mAs at 1m)	HVL (mm Al)	kV T/F	Output (mGy/mAs at 1m)	HVL (mm Al)
25 W/Rh	11.2	0.48	25 W/Ag	12.6	0.49
28 W/Rh	15.7	0.51	28 W/Ag	18.4	0.54
31 W/Rh	20.1	0.54	31 W/Ag	24.2	0.58
34 W/Rh	24.4	0.56	34 W/Ag	29.8	0.61
37 W/Rh	28.6	0.59	37 W/Ag	35.4	0.64

3.2 Detector response

The detector was found to have a linear response, with an offset of 50, as shown in Figure 3.

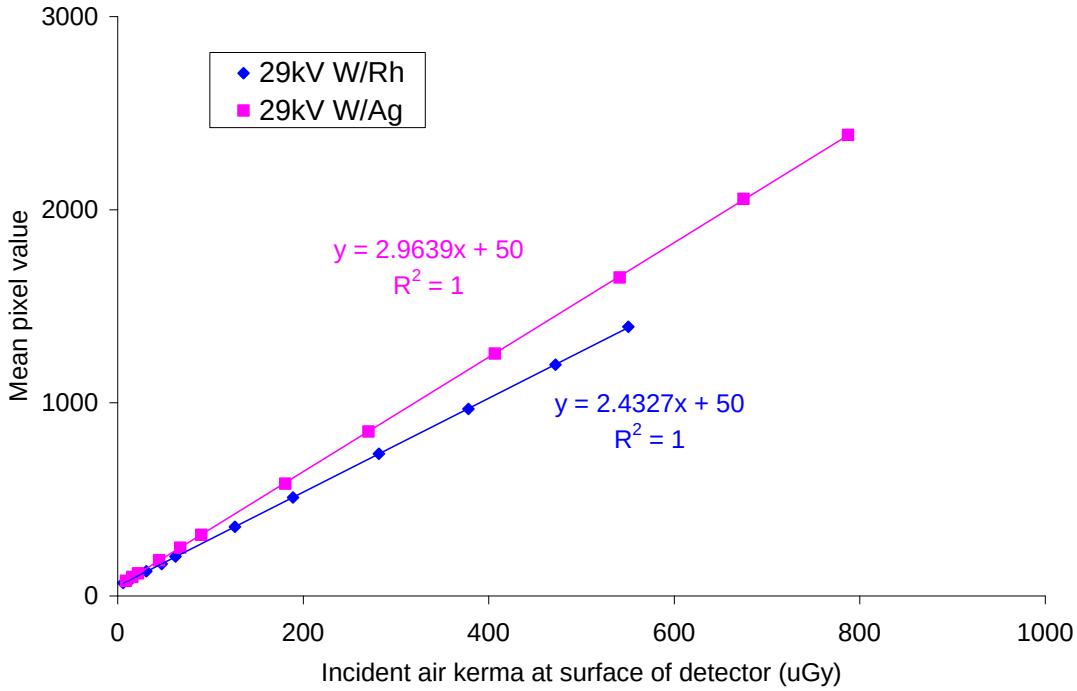

Figure 3 Detector response.

3.3 AEC performance

3.3.1 Dose

The mean glandular doses for breasts simulated with PMMA and exposed under AEC control are shown in Table 5 and Figure 4. At all thicknesses, the dose was below the remedial level given in the NHSBSP protocol, which is the same as the maximum acceptable level in the European Protocol. The 'displayed MGD' values in Table 5 are calculated according to Wu et al.[8], and are not expected to be identical to the MGD values presented in column 8 of Table 5, which are calculated according to Dance et al.[9] (Values calculated according to Wu et al. are expected to be about 10% lower than those calculated according to Dance et al.)

The main effect of the AEC software upgrade was to increase the MGDs (and CNRs) for larger breasts. The MGD for 53 mm PMMA thickness (1.36 mGy) was found to be slightly lower than the target value of 1.42 mGy supplied by Hologic, but was within tolerance limits.

The pre-exposure pulse used in AEC modes is 5 mAs for compressed breast thicknesses of less than 50 mm, and 10 mAs for thicknesses equal to or greater than 50 mm. This contributes to the mean glandular dose, but is not used to produce the digital image.

Table 5 Mean glandular dose for simulated breasts (AutoFilter mode)

PMMA thickness (mm)	Equivalent breast thickness (mm)	kV	Target	Filter	mAs*	MGD before upgrade (mGy)	MGD after upgrade (mGy)	% Increase in MGD	NHSBSP remedial level (mGy)	Displayed MGD (mGy)
20	21	25	W	Rh	45	0.57	0.55	4	>1.0	0.56
30	32	26	W	Rh	69	0.80	0.79	1	>1.5	0.78
40	45	28	W	Rh	90	1.09	1.19	-8	>2.0	1.05
45	53	29	W	Rh	108	1.36	1.40	-3	>2.5	1.27
50	60	31	W	Rh	131	1.87	1.65	13	>3.0	1.72
60	75	31	W	Ag	156	2.51	1.85	36	>4.5	2.29
70	90	34	W	Ag	154	2.89	2.26	28	>6.5	2.65

*mAs values here include pre-exposure mAs, as this contributes to the MGD.

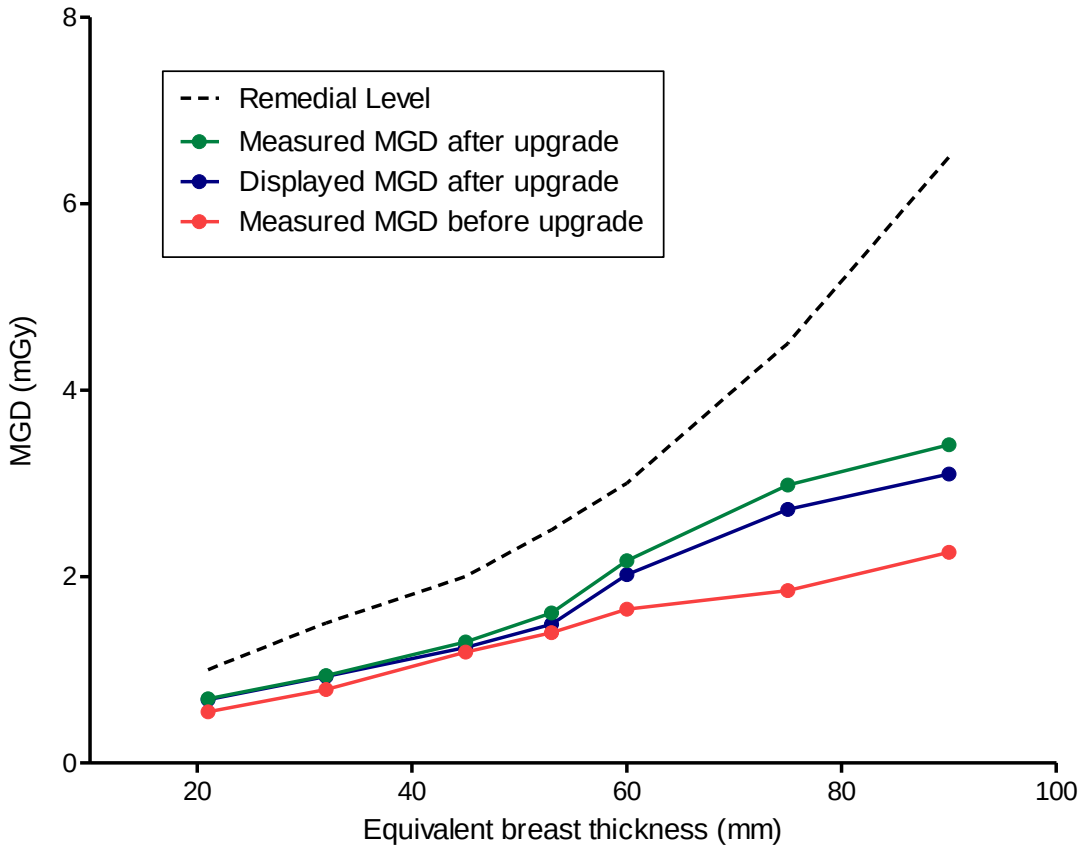

Figure 4 MGD for different thicknesses of simulated breasts using the AutoFilter mode.

3.3.2 CNR

The results of the contrast and CNR measurements are shown in Table 6 and Figure 5. The CNRs that are required to meet the minimum acceptable and achievable image quality standards at the 60 mm breast thickness are shown, along with the CNR required at each thickness to meet the limiting values for CNR in the European protocol.

Table 6 Contrast and CNR measurements using AEC

Equivalent breast thickness (mm)	*kV target/ filter*	*mAs**	*Back-ground pixel value*	*% contrast for 0.2 mm Al*	*Measured CNR*	*CNR at minimum acceptable IQ*	*CNR at achievable IQ*	*CNR to meet European limiting value*	*European limiting values for relative CNR*
21	25 W/Rh	45	321	20.10%	10.55	3.85	5.69	4.43	>115
32	26 W/Rh	69	321	18.90%	9.52	3.85	5.69	4.24	>110
45	28 W/Rh	90	321	16.90%	8.39	3.85	5.69	4.05	>105
53	29 W/Rh	108	332	16.10%	8.13	3.85	5.69	3.97	>103
60	31 W/Rh	131	419	14.20%	8.13	3.85	5.69	3.86	>100
75	31 W/Ag	156	553	12.00%	7.74	3.85	5.69	3.66	>95
90	34 W/Ag	154	569	9.90%	6.42	3.85	5.69	3.47	>90

*mAs values here do not include pre-exposure mAs, as this does not contribute to the image.

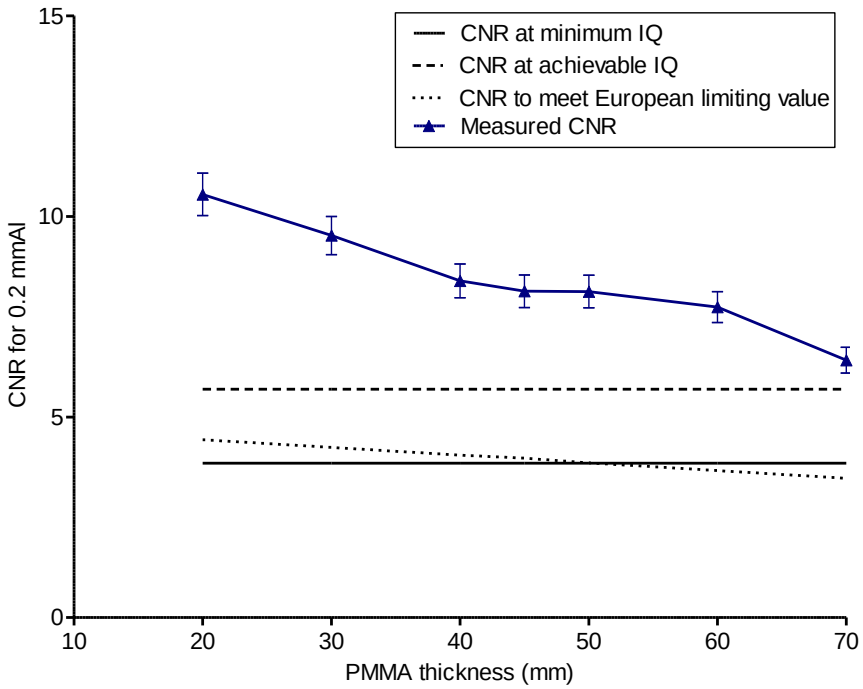

Figure 5 Measured CNR compared with the limiting values in the European protocol for the system. (Error bars indicate 95% confidence limits.)

3.3.3 AEC performance for local dense areas

It is expected that when the AEC adjusts for locally dense areas, the SNR will remain constant in that area as extra PMMA layers are added, as shown in Table 7 and Figure 6.

Table 7 AEC performance for local dense areas (AutoFilter mode)

Attenuation (mm PMMA)	Target/ filter	Tube voltage (kV)	Tube load (mAs)	SNR
32	W/Rh	28	51	53.1
34	W/Rh	28	65	56.8
36	W/Rh	28	73	56.1
38	W/Rh	28	82	56.9
40	W/Rh	28	93	58.5
42	W/Rh	28	104	58.1
44	W/Rh	28	115	55.7
46	W/Rh	28	131	58.6
48	W/Rh	28	144	57.4

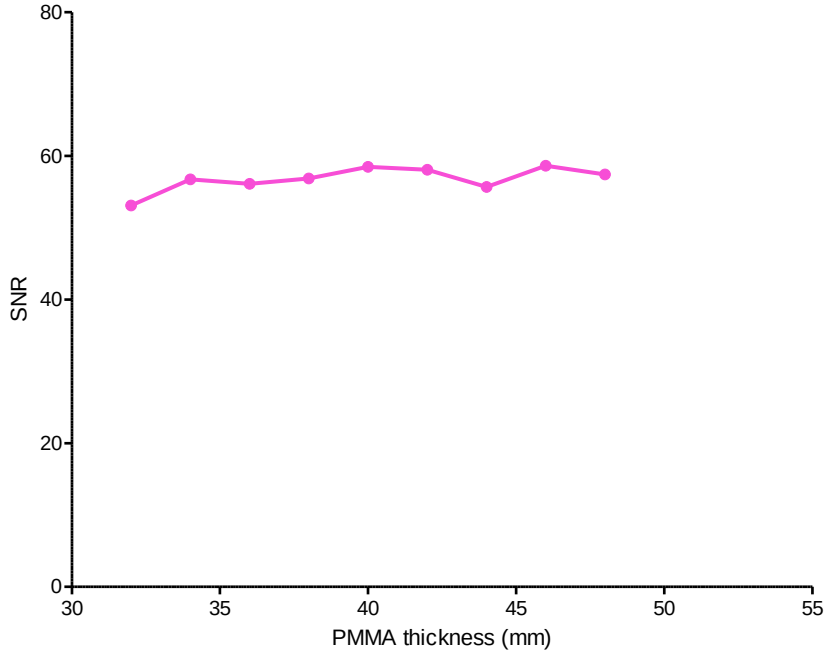

Figure 6 AEC performance for local dense areas.

3.4 Noise measurements

The variation in noise with dose was analysed by plotting the standard deviation in pixel values against the detector entrance air kerma, as shown in Figure 7. The fitted power curve has an index of 0.44. If quantum noise sources alone were present, the data would form a straight line with an index of 0.5. The data deviates from a straight line at lower doses owing to the presence of electronic noise. This is normal for such systems. Quantum noise was the dominant noise source.

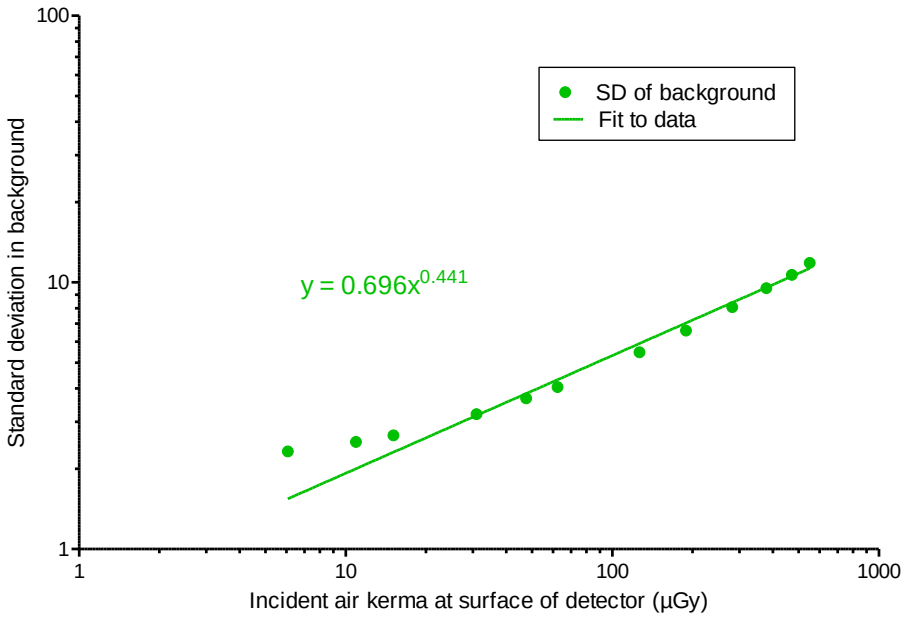

Figure 7 Standard deviation of pixel values versus air kerma at detector.

Figure 8 is an alternative way of presenting the data and shows the relative noise at different entrance air kerma. The estimated relative contributions of electronic, structural, and quantum noise are shown and the quadratic sum of these contributions fitted to the measured noise (using Equation 3). Figure 9 shows the different amounts of variance caused by each component. Quantum noise predominates over the clinical range.

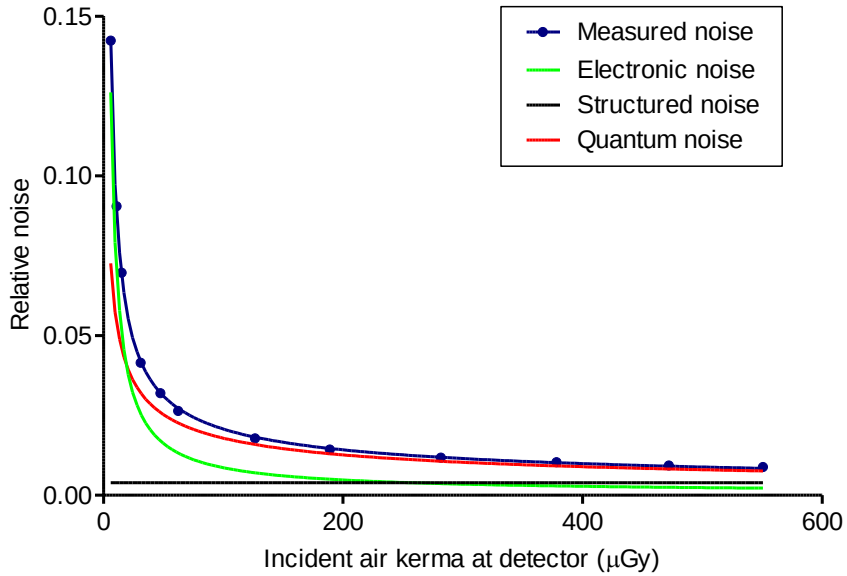

Figure 8 Relative noise and noise components at different pixel values.

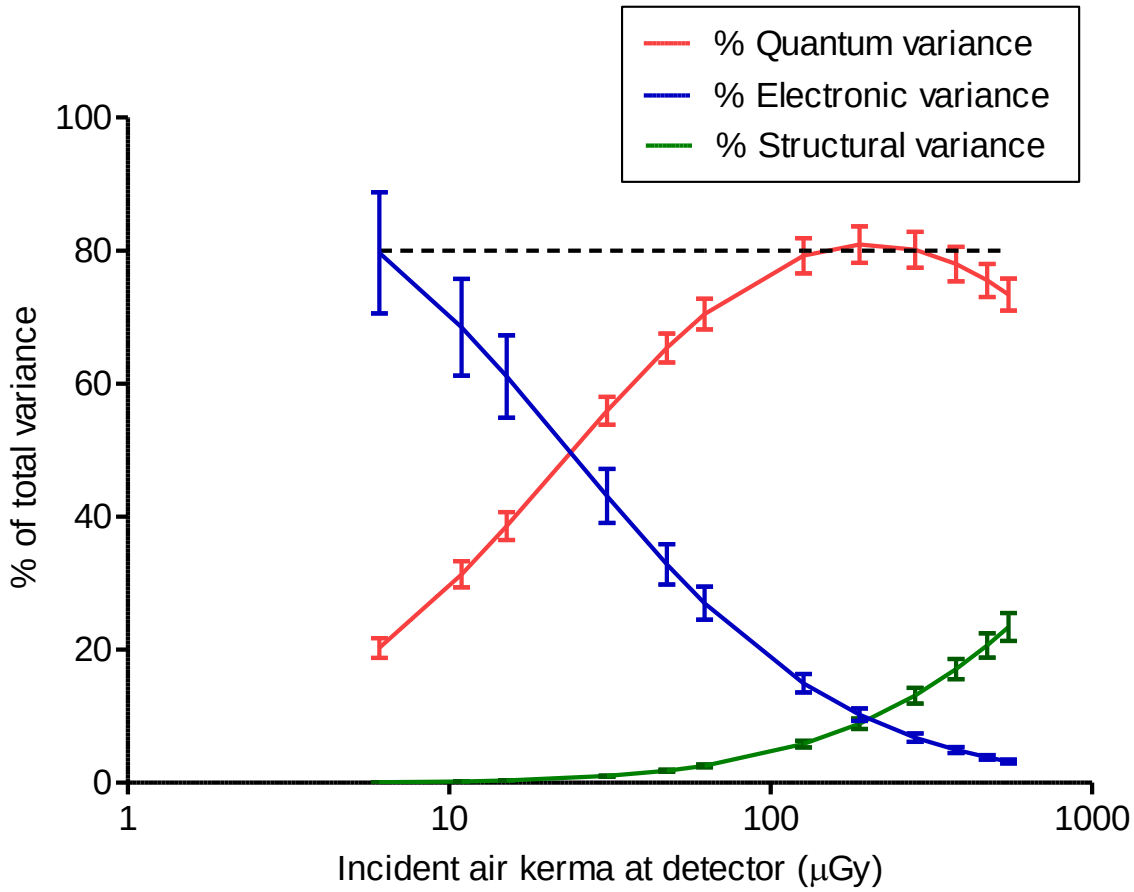

Figure 9 Each noise component as a percentage of the total variance. The percentage quantum variance is compared with a limit of 80%. Error estimates are based on the assumption that the errors in each of the components were independent. (Error bars indicate 95% confidence limits.)

3.5 Image quality measurements

The first exposure of the image quality phantom was made using the AEC in standard mode to select the beam quality and exposure factors. This resulted in the selection of 31 kV W/Rh and 130 mAs and an MGD of 1.84 mGy to an equivalent breast (60 mm thick). Subsequent image quality measurements were made by manual selection, at a range of mAs values between approximately half and double the AEC-selected mAs, and at the same beam quality as shown in Table 8.

Table 8 Images acquired for image quality measurement

Exposure mode	kV target/filter	Tube loading (mAs)	Mean glandular dose to equivalent breasts 60mm thick (mGy)	Number of CDMAM images acquired and analysed
Manual	31 kV W/Rh	65	0.93	15
Manual	31 kV W/Rh	80	1.14	15
Manual	31 kV W/Rh	125	1.78	15
Manual	31 kV W/Rh	150	2.14	16
Manual	31 kV W/Rh	200	2.85	15
Manual	31 kV W/Rh	250	3.56	15

The contrast detail curves at the different dose levels (determined by automatic reading of the images) are shown in Figure 10. The threshold gold thicknesses for different diameters and the different dose levels for the two systems are shown in Table 9, along with the minimum and achievable threshold values from the NHSBSP protocol (which are the same as those of the European protocol). The data in Table 9 are taken from the fitted curves rather than the raw data.

The measured threshold gold thicknesses are plotted against the MGD for an equivalent breast for the 0.1 and 0.25 mm detail sizes in Figure 11. The curves in Figure 11 were interpolated to find the doses required to meet the minimum acceptable and achievable threshold gold thicknesses in Table 9, and the results are shown in Tables 10 and 11. A similar procedure was used to determine the doses required to meet the minimum acceptable and achievable image quality levels for detail sizes from 0.1 to 1.0 mm, as shown in Figure 12.

Table 9 Average threshold gold thicknesses for different detail diameters for three doses using 31 kV W/Rh and automatically predicted data

			Threshold gold thickness (µm)					
Diameter (mm)	Acceptable value	Achievable value	MGD = 0.93 mGy	MGD = 1.14 mGy	MGD = 1.78 mGy	MGD = 2.14 mGy	MGD = 2.85 mGy	MGD = 3.56 mGy
0.1	1.68	1.1	1.105 ± 0.085	0.911 ± 0.070	0.744 ± 0.057	0.616 ± 0.043	0.591 ± 0.045	0.554 ± 0.042
0.25	0.352	0.244	0.243 ± 0.018	0.245 ± 0.019	0.191 ± 0.015	0.174 ± 0.013	0.157 ± 0.012	0.141 ± 0.011
0.5	0.15	0.103	0.106 ± 0.009	0.109 ± 0.009	0.082 ± 0.007	0.079 ± 0.006	0.067 ± 0.006	0.060 ± 0.005
1	0.091	0.056	0.055 ± 0.006	0.056 ± 0.006	0.042 ± 0.005	0.041 ± 0.005	0.035 ± 0.004	0.033 ± 0.004

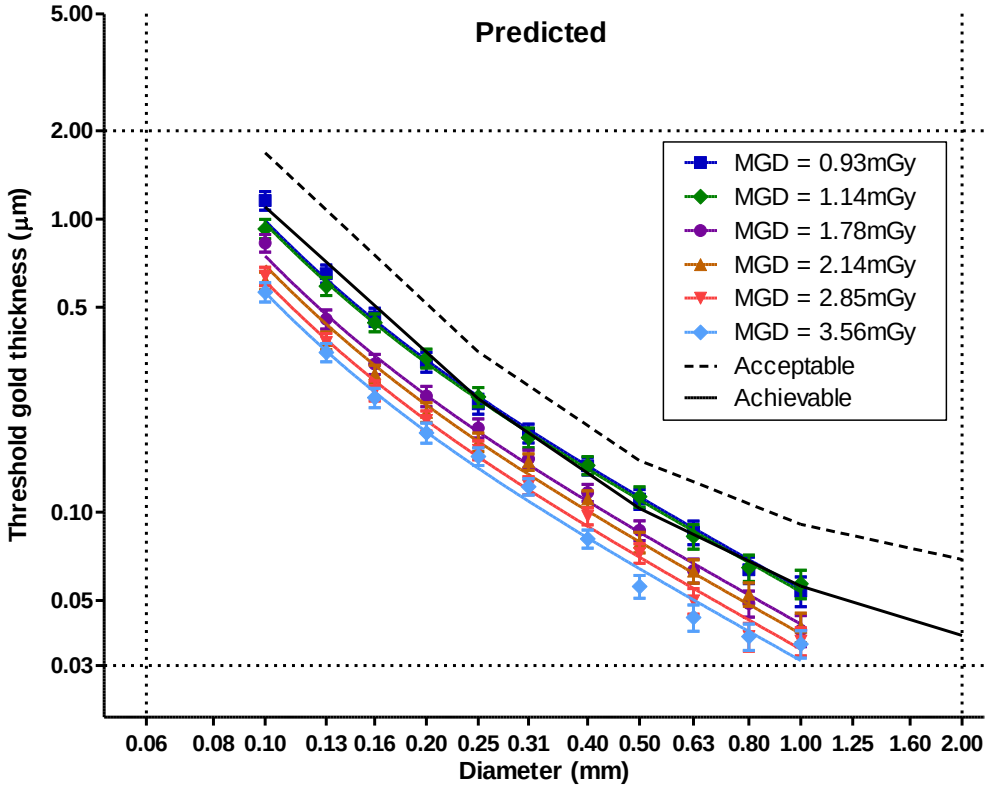

Figure 10 Contrast detail curves for six doses at 31 kV W/Rh using predicted results from automated reading. The 1.78 mGy dose corresponds to the AEC selection. (Error bars indicate 95% confidence limits.)

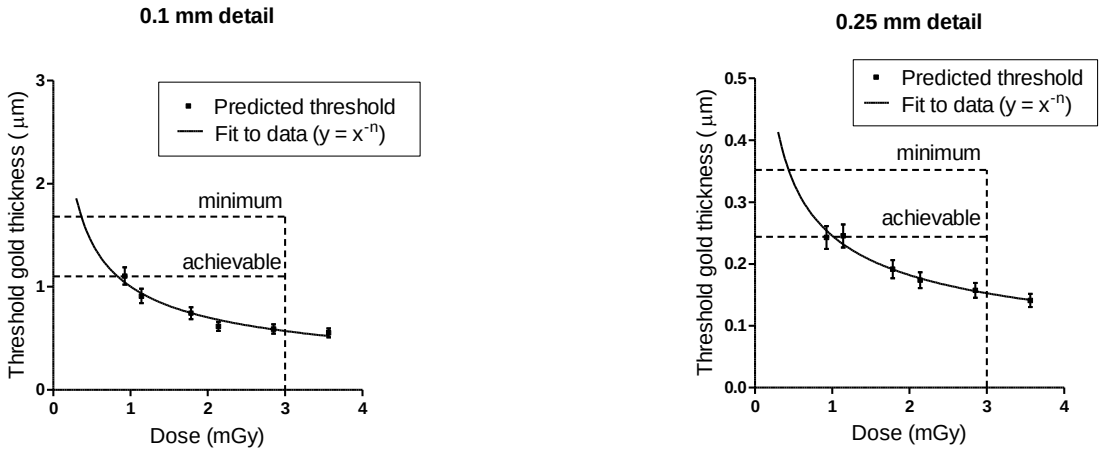

Figure 11 Threshold gold thickness at different doses. (Error bars indicate 95% confidence limits.) The doses are for a breast equivalent to a 5 cm thickness of PMMA.

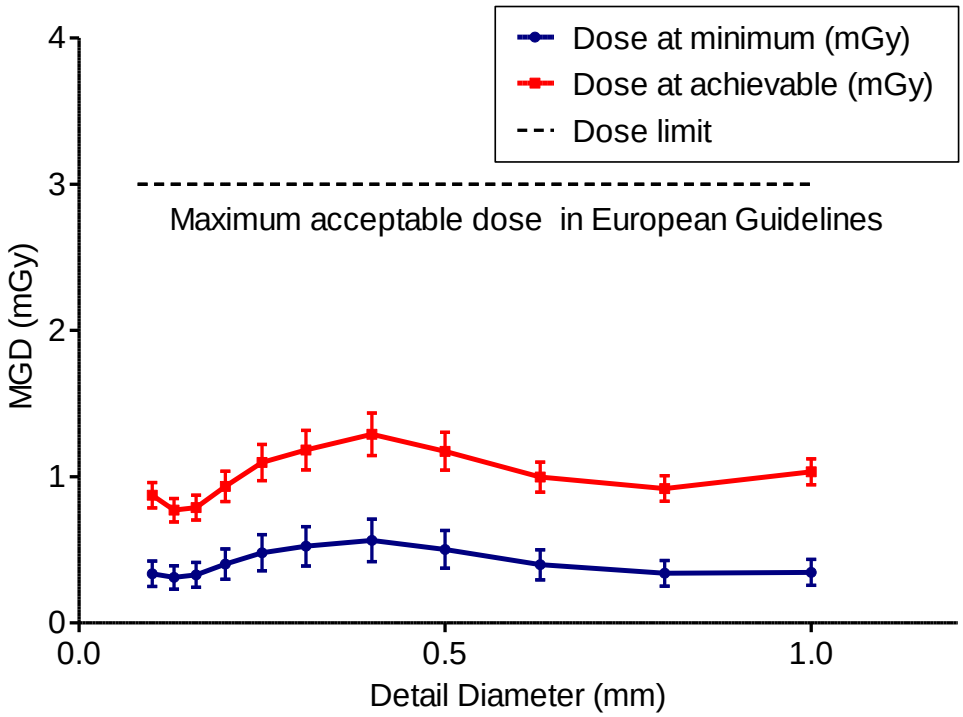

Figure 12 The MGD calculated to be necessary to reach the achievable and minimum acceptable image quality levels at different detail sizes using 31 kV W/Rh for an equivalent breast 60 mm thick (based on predicted threshold gold thicknesses). (Error bars indicate 95% confidence limits.)

3.6 Comparison with other systems

The MGDs required to reach the minimum and achievable image quality standards in the NHSBSP protocol have been estimated from the curves shown in Figure 11. (The error in estimating these doses depends on the accuracy of the fitting procedure for the curve and pooled data for several systems has been used to estimate the 95% confidence limits of around 20%). These doses are shown against similar data for other models of digital mammography system in Tables 10 and 11, and Figures 13 to 16. The data for the other systems has been determined in as described in this report and the results published previously.[4,10-21] The data for film screens represent an average value, which was determined using a variety of modern film screen systems.

Table 10 The MGD required to reach the minimum threshold gold thickness for 0.1 and 0.25 mm details for different systems

	MGD (mGy) for 0.1 mm		MGD (mGy) for 0.25 mm	
System	Human	Predicted	Human	Predicted
Sectra MDM-L30	0.41		0.41	0.42
Siemens Novation*	0.54	0.59	0.47	0.67
Siemens Inspiration	0.97	0.76	0.87	0.60
Fuji Amulet	0.62	0.67	0.74	0.71
Hologic Dimensions v1.4.2		0.34		0.48
Hologic Dimensions	0.56	0.38	0.65	0.40
Hologic Selenia (Mo)	0.85	0.55	0.80	0.53
Hologic Selenia (W)	0.58	0.71	0.65	0.64
GE Essential	0.60	0.49	0.50	0.49
GE DS	1.01	0.82	0.87	0.83
IMS Giotto (W)	1.07	1.38	0.91	1.17
Film-screen	1.17	1.30	1.07	1.36
Agfa CR85-X (NIP)	1.24	1.27	1.06	0.96
Agfa CR (MM3.0)†	2.54	2.32	1.45	1.54
Fuji Profect CR	1.67	1.78	1.45	1.35
Carestream CR (EHR-M2)	2.29	2.34	1.45	1.80
Konica Minolta (CP-1M)	1.60	1.47	1.12	0.99

*Data are the mean of measurements for two systems in NHSBSP Equipment Report 0710.[14]

†Data are the mean of measurements shown in NHSBSP Equipment Reports 0707[13] and 0905.[20]

Table 11 The MGD required to reach the achievable threshold gold thickness for 0.1 and 0.25 mm details for different systems.

	MGD (mGy) for 0.1 mm		MGD (mGy) for 0.25 mm	
System	Human	Predicted	System	Human
Sectra MDM	1.27	1.74	1.37	0.95
Siemens Novation‡	1.30	1.26	1.00	1.37
Siemens Inspiration	2.06	1.27	1.68	1.16
Fuji Amulet	1.40	1.13	1.50	1.41
Hologic Dimensions v1.4.2		0.87		1.10
Hologic Dimensions	1.29	0.91	1.23	0.85
Hologic Selenia (Mo)	1.84	1.19	1.68	1.12
Hologic Selenia (W)	1.66	1.37	1.61	1.48
GE Essential	1.57	1.13	1.14	1.03
GE DS	2.35	1.57	1.80	1.87
IMS Giotto (W)	2.33	2.73	1.77	2.11
Film-screen	2.48	3.03	2.19	2.83
Agfa CR (NIP)	3.22	2.47	2.40	2.34
Agfa CR (MM3.0)§	5.21	5.14	3.72	3.82
Fuji Profect CR	4.26	3.29	3.52	2.65
Carestream CR (EHR-M2)	5.34	5.45	3.03	3.74
Konica Minolta CR (CP-1M)	4.53	3.45	2.73	2.08

‡ Data are the mean of measurements for two systems in NHSBSP Equipment Report 0710.[14] § Data are the mean of measurements shown in NHSBSP Equipment Reports 0707[13] and 0905.[20]

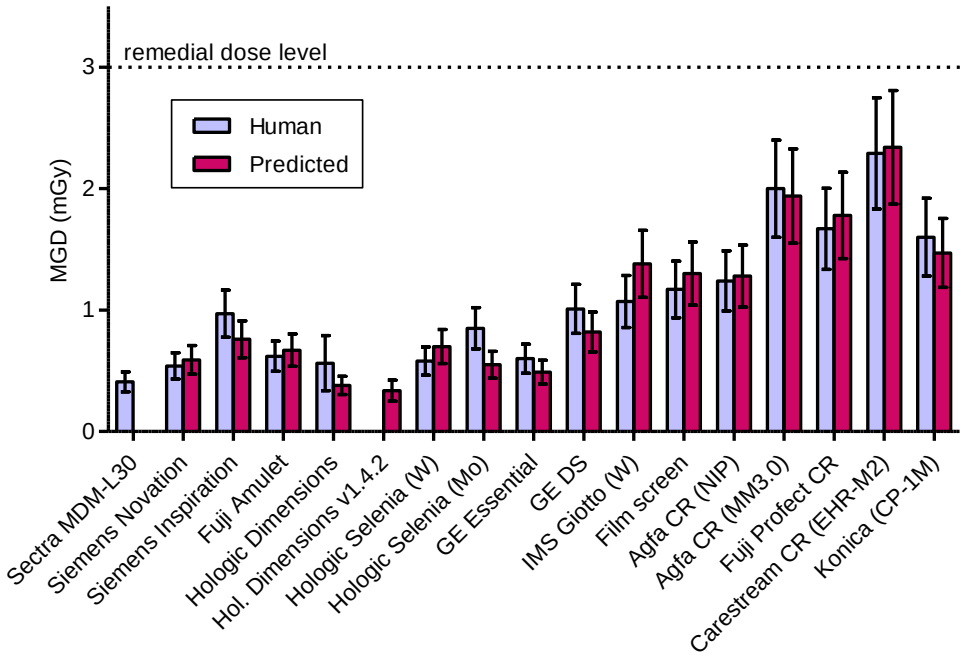

Figure 13 Dose to reach minimum acceptable image quality standard for 0.1 mm detail. (Error bars indicate 95% confidence limits).

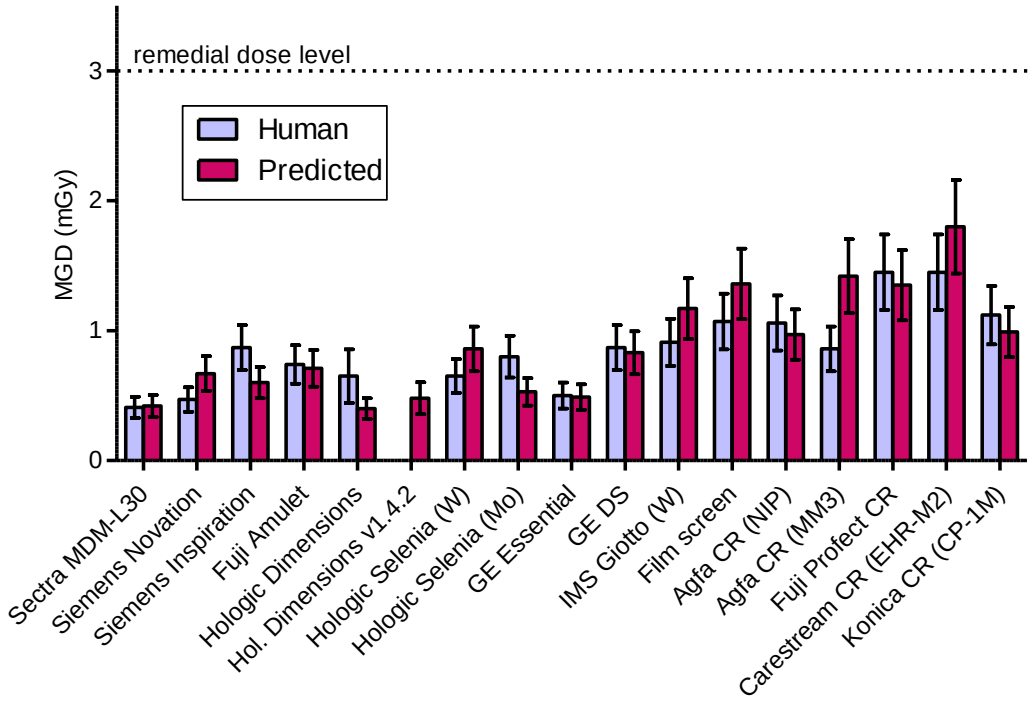

Figure 14 Dose to reach minimum acceptable image quality standard for 0.25 mm detail. (Error bars indicate 95% confidence limits).

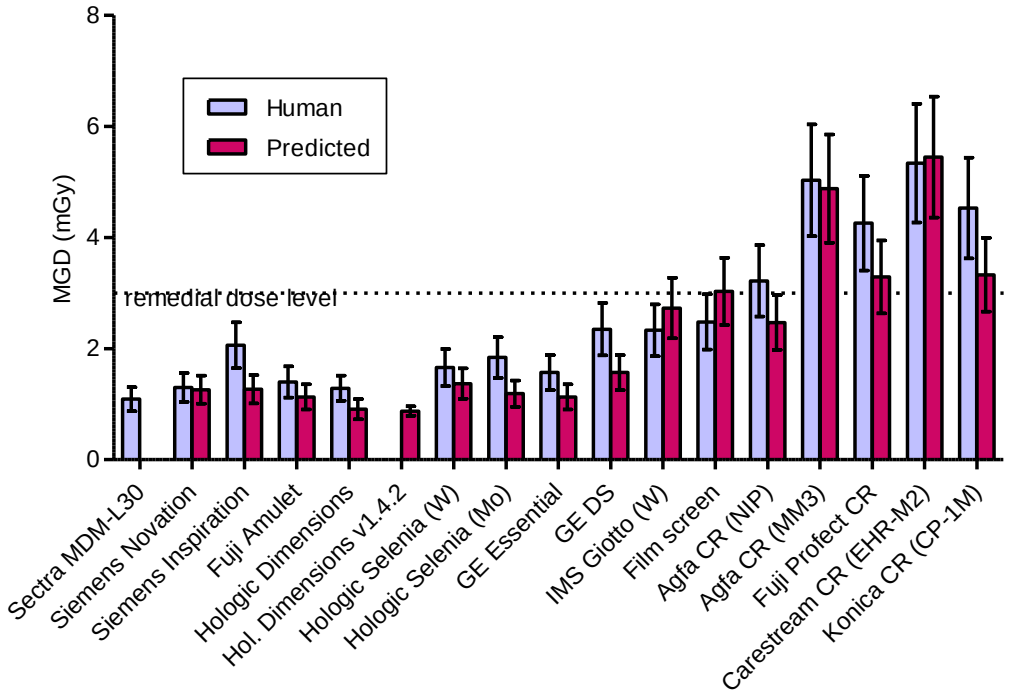

Figure 15 Dose to reach achievable image quality standard for 0.1 mm detail. (Error bars indicate 95% confidence limits)

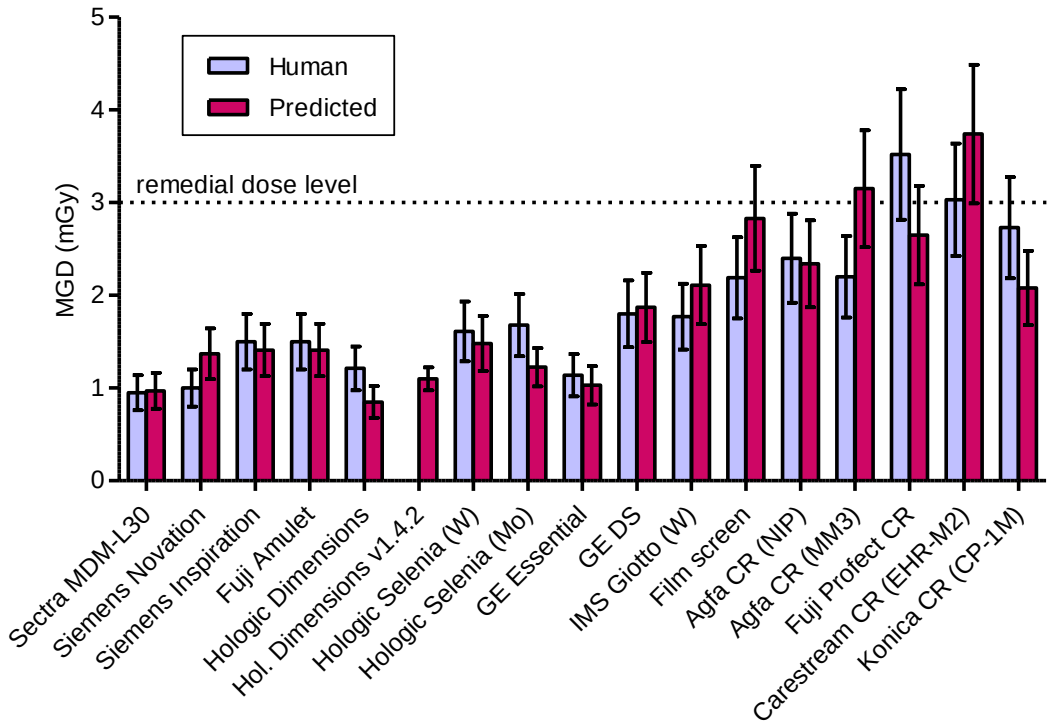

Figure 16 Dose to reach achievable image quality standard for 0.25 mm detail. (Error bars indicate 95% confidence limits

3.7 Artefact

While a raw image (Figure 17) shows no black surrounding area around the metal coil, this artefact is clearly present in the processed image before the software upgrade (Figure 18). It is not present in the processed image after the upgrade (Figure 19).

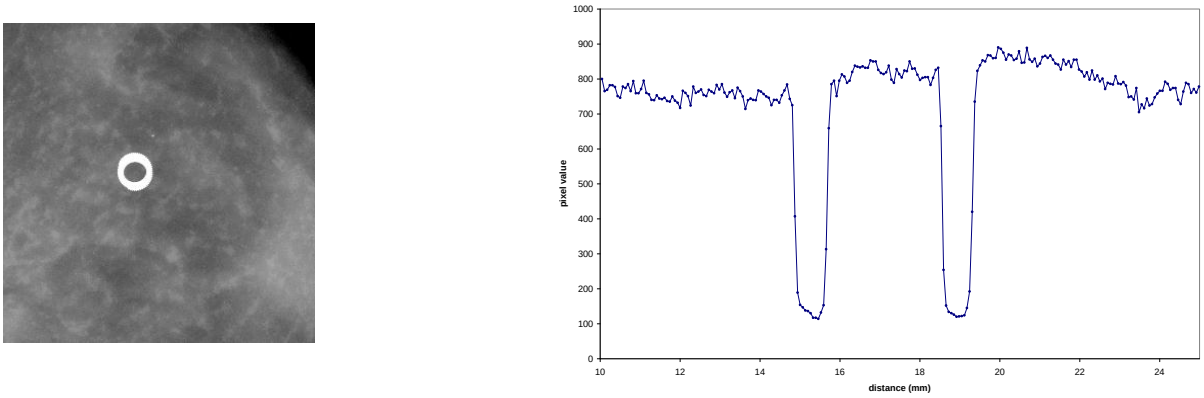

Figure 17 Raw image of a small metal coil on a breast phantom and a profile across the image.

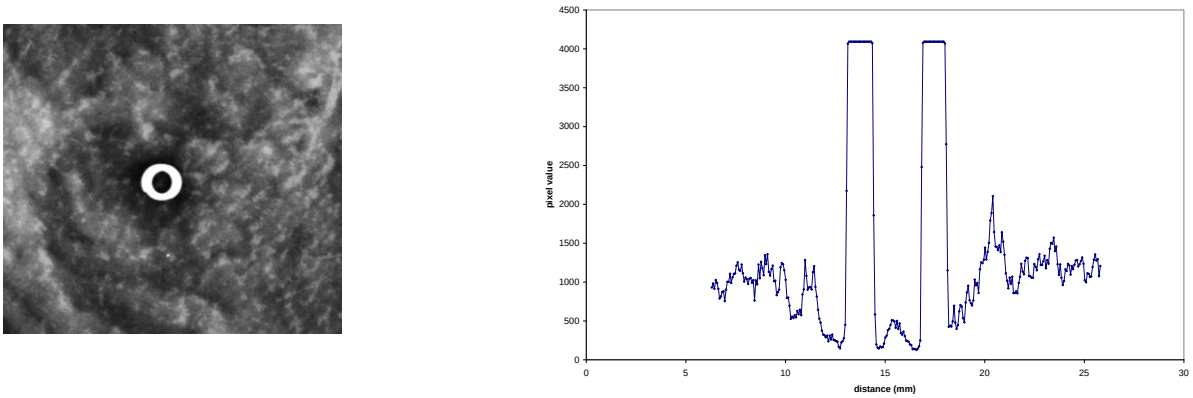

Figure 18 Processed image (before software upgrade) of a small metal coil on a breast phantom and a profile across the image. The black area in and around the white ring is an artefact. The minimum pixel value is approximately 150.

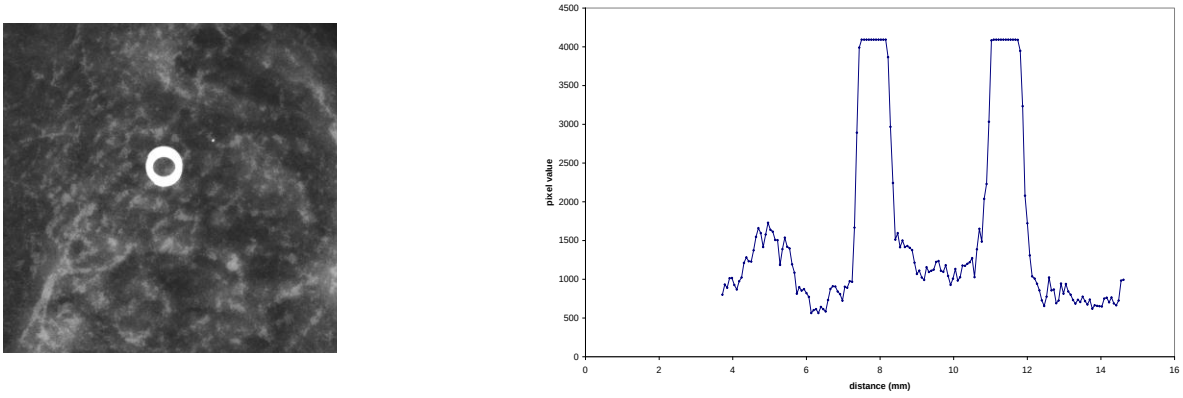

Figure 19 Processed image (after software upgrade) of a small metal coil on a breast phantom and a profile across the image. The minimum pixel value is approximately 500.

4. DISCUSSION

The performance of the system (with software upgrade version 1.4 installed) was satisfactory.

The MGDs for different thicknesses of PMMA have increased by 13-36% for greater thicknesses (5-7 cm PMMA), compared with the previous values for the same unit. For smaller thicknesses the changes were less than 10%. The new MGDs were well below the remedial level, standing at (for example) .36 mGy (target value 1.42 mGy) for the equivalent standard breast (45 mm PMMA), which is low compared with the remedial level of 2.5 mGy.

Image quality after the upgrade was found to be better than the “achievable” level using the AEC settings. The measured CNR values were well above the values corresponding to achievable image quality for all thicknesses. The new software has improved image quality for thicker breasts for a slight increase in dose.

On the upgraded system there was no evidence of an artefact (dark area) around the image of a metal coil on a breast-like phantom background. The artefact had been clearly present before the upgrade.

5. CONCLUSIONS

The system met the main standards of the NHSBSP and European protocols.

6. REFERENCES

1. *Commissioning and Routine Testing of Full Field Digital Mammography Systems* (NHSBSP Equipment Report 0604). Sheffield: NHS Cancer Screening Programmes, 2006.
2. Young K C, Johnson B, Bosmans H, et al. R. Development of minimum standards for image quality and dose in digital mammography. In: Pisano E (ed) *Proceedings of the 7th International Workshop on Digital Mammography (2004)*, 2005, 149-154.
3. Van Engen R, Young K C, Bosmans H, et al. The European protocol for the quality control of the physical and technical aspects of mammography screening. In: *European Guidelines for Quality Assurance in Breast Cancer Screening and Diagnosis*, 4th Edition. Luxembourg: European Commission, 2006.
4. *Technical Evaluation of the Hologic Selenia Dimensions 2-D Digital Breast Imaging System* (NHSBSP Equipment Report 1101). Sheffield: NHS Cancer Screening Programmes, 2011.
5. Alsager A, Young K C, Oduko J M. Impact of Heel Effect and ROI Size on the Determination of Contrast-to-Noise Ratio for Digital Mammography Systems. In: *Proceedings of SPIE Medical Imaging*. Bellingham WA: SPIE Publications, 2008, 69134I: 1-11.
6. Young K C, Cook J J H, Oduko J M. Automated and human determination of threshold contrast for digital mammography systems. In Astley S M, Bradley M, Rose C (eds) *Proceedings of the 8th International Workshop on Digital Mammography.* Berlin: Springer-Verlag, 2006, 4046: 266-272.
7. Young K C, Alsager A, Oduko J M et al. Evaluation of software for reading images of the CDMAM test object to assess digital mammography systems. In: *Proceedings of SPIE Medical Imaging*. Bellingham WA: SPIE Publications, 2008, 69131C: 1-11.
8. Wu X, Gingold E L, Barnes G T, et al. Normalized average glandular dose in molybdenum target-rhodium filter and rhodium target-rhodium filter mammography. *Radiology,* 1994, 193(1): 83–9 .
9. Dance D R, Young K C, Van Engen R E. Further factors for the estimation of mean glandular dose using the United Kingdom, European and IAEA breast dosimetry protocols. *Physics in Medicine and Biology,* 2009, 54: 4361-4372.
10. *Evaluation of Kodak DirectView Mammography Computerised Radiography* (NHSBSP Equipment Report 0504). Sheffield: NHS Cancer Screening Programmes, 2005
11. *Technical Evaluation of the Hologic Selenia Full Field Digital Mammography System* (NHSBSP Equipment Report 0701). Sheffield: NHS Cancer Screening Programmes, 2007
12. *Technical Evaluation of Kodak DirectView Mammography Computerised Radiography System Using EHR-M2 Plates* (NHSBSP Equipment Report 0706). Sheffield: NHS Cancer Screening Programmes, 2007.
13. *Technical Evaluation of the Agfa CR85-X Mammography System* (NHSBSP Equipment Report 0707). Sheffield: NHS Cancer Screening Programmes, 2007.

14. *Technical Evaluation of the Siemens Novation Full Field Digital Mammography System* (NHSBSP Equipment Report 0710). Sheffield: NHS Cancer Screening Programmes, 2007.

15. *Technical Evaluation of the Hologic Selenia Full Field Digital Mammography System with a Tungsten Tube* (NHSBSP Equipment Report 0801). Sheffield: NHS Cancer Screening Programmes, 2008 .

16. *Technical Evaluation of the GE Essential Full Field Digital Mammography System* (NHSBSP Equipment Report 0803). Sheffield: NHS Cancer Screening Programmes, 2008.

17. *Technical Evaluation of the IMS Giotto Full Field Digital Mammography System with a Tungsten Tube* (NHSBSP Equipment Report 0804). Sheffield: NHS Cancer Screening Programmes, 2008.

18. *Technical Evaluation of the Konica Minolta Regius 190 CR Mammography System and Three Types of Image Plate* (NHSBSP Equipment Report 0806). Sheffield: NHS Cancer Screening Programmes, 2008.

19. *Technical Evaluation of Profile Automatic Exposure Control Software on GE Essential Full Field Digital Mammography System* (NHSBSP Equipment Report 0903). Sheffield: NHS Cancer Screening Programmes, 2009.

20. *Technical Evaluation of Agfa DX-M Mammography CR Reader with HM5.0 Needle-IP* (NHSBSP Equipment Report 0905). Sheffield: NHS Cancer Screening Programmes, 2009.

21. *Technical Evaluation of Fuji Amulet Full Field Digital Mammography System* (NHSBSP Equipment Report 0907). Sheffield: NHS Cancer Screening Programmes, 2009.

NHS Cancer Screening Programmes
Fulwood House
Old Fulwood Road
Sheffield
S10 3TH

July 2012